MIDWESTERN UNIVERSITIES RESEARCH ASSOCIATION

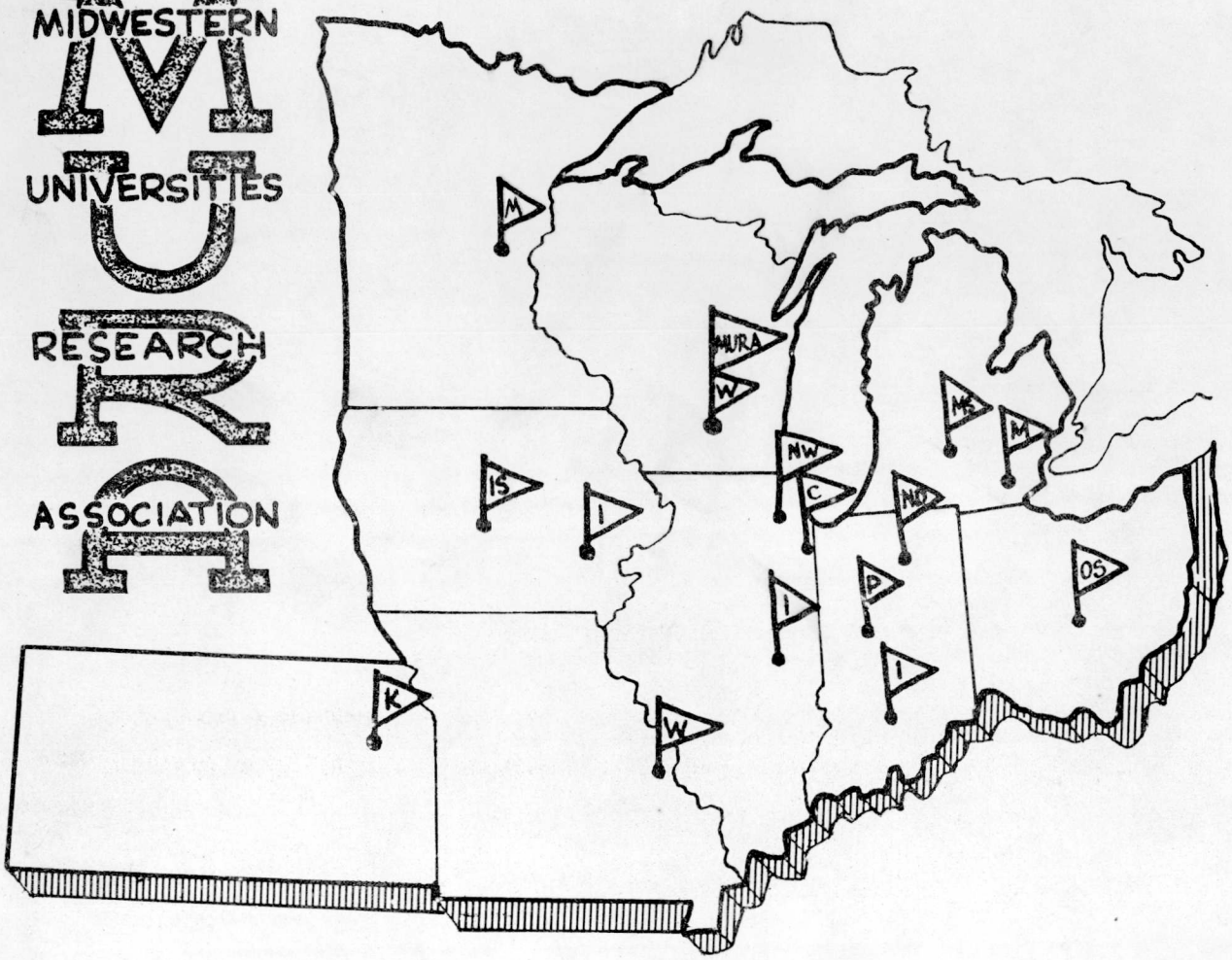

ON THE TWO-BEAM FFAG ACCELERATOR

Tihiro Ohkawa

REPORT NUMBER 318

MIDWESTERN UNIVERSITIES RESEARCH ASSOCIATION*

2203 University Avenue, Madison, Wisconsin

ON THE TWO-BEAM FFAG ACCELERATOR

Tihiro Ohkawa**

July 5, 1957

ABSTRACT

Analytical expressions for the orbits and the linear betatron oscillations of the two-beam FFAG accelerator are given and compared with the results obtained by the digital computer. Typical design parameters are discussed.

* Supported by Contract AEC #AT (11-1)-384

** On leave from the University of Tokyo

INTRODUCTION

As pointed out by the MURA group,[1] the method of achieving very high energy collisions between elementary particles by means of colliding beams appears highly promising if the potential high intensity of the FFAG accelerators is realized. As first envisaged, a colliding beam accelerator would consist of two FFAG accelerators tangent to one another. An alternative method[2],[3] employing a pulsed accelerator and storage rings has been proposed by D. Lichtenberg and G.K. O'Neill.

This report concerns the proposed new colliding beam method,[4],[5] where both beams are in the same accelerator, circulating in opposite directions. Since this method employs a single accelerator, the troublesome problems in the other methods, such as target sections having inherently non-scaling features and beam transfer (usually not too efficient), can be avoided.

The machine is essentially a radial sector FFAG machine and has a fairly large circumference factor. However the simple structure of the magnets compared to two spiral machines, the many intersections of beams for experiments and the feasibility of changing the reaction energy make the machine an interesting possibility.

- - - - - - - - - - - - - - -

(1) D.W. Kerst et al Phy. Rev. 102 No. 2, 1956

(2) D. Lichtenberg et al MURA-DBL/RAN/HMR-1

(3) G.K. O'Neill Phy. Rev. 102 1418 (1956)

(4) T. Ohkawa, MURA-124

(5) L.W. Jones, MURA-134

GENERAL DESCRIPTION OF THE MAGNETIC FIELD

In the magnetic fields of FFAG accelerators, there exist an infinite number of equilibrium orbits due to the nonlinearity of the field. However these orbits have extremely large circumference factors, except two orbits which are clockwise and anticlockwise respectively in a radial sector machine. These two orbits generally have different properties, such as the circumference factor and the tunesof the betatron oscillations. The one which is not used in an ordinary radial sector machine is usually unstable. We are interested here in making these two orbits cross each other at an equal energy of particles and work at the same point on the tune diagram. This can be achieved by using a magnetic field having a certain symmetry property.

We write the median plane field as

$$H_{z0} = -H_0 \left(\frac{r}{r_0}\right)^k f(N\theta) \tag{1}$$

where

$$f(N\theta + 2\pi) = f(N\theta)$$

The Lagrangian for the motion in the median plane is given by

$$\mathcal{L} = \pm p\sqrt{r^2 + r'^2} + \frac{e}{c} r A_{\theta 0} \tag{2}$$

where

$$\frac{e}{c} r A_{\theta 0} = -\frac{e}{c} H_0 \frac{1}{k+2} \frac{r^{k+2}}{r_0^k} f(N\theta), \tag{3}$$

primes denote derivatives with respect to θ and $\pm$ is chosen depending on the direction of rotation.

It is obvious from the Lagrangian (1) that the condition for obtaining the identical two-way orbits is to make $f(N\theta)$ an odd function of $N\theta$, i.e.

$$f(-N\theta) = -f(N\theta) \tag{4}$$

because the equation of motion is identical for both directions if $f(N\theta)$ satisfies (4).

By rewriting $f(N\theta)$ in Fourier series form

$$f(N\theta) = \sum_n \left(g_n \cos nN\theta + f_n \sin nN\theta \right) \tag{5}$$

(4) implies

$$g_n = 0 \qquad \text{for all } n \tag{6}$$

Customarily we put $N\theta = 0$ at the middle of the "positive magnet" and (5) and (6) become

$$f(N\theta) = f_1 \cos N\theta - f_2 \sin 2N\theta + f_3 \cos 3N\theta - \cdots\cdots \tag{7}$$

by putting $N\theta \rightarrow N\theta + \frac{\pi}{2}$

Especially if all even f's vanish, (7) becomes

$$f(N\theta) = \sum f_{2j+1} \cos(2j+1)N\theta \tag{8}$$

and we have an additional symmetry around the middle of the positive magnet.

From the results of rough estimate of the orbits and the betatron oscillations around them, it is realized that the contributions from higher harmonics

of the field depend on a quantity $\sum \frac{f_{j'}^2}{j'^2}$ except for the axial focusing, which depends also on $\sum f_{j'}^2$ In actual fields, the higher harmonic content is not very high. For example, $f_{2j'+1}$ is given by $\frac{1}{2j'+1}$ for a rectangular-shaped field. Therefore, to understand the behavior of the machine, a pure sinusoidal field is not a poor choice.

ORBITS

The Lagrangian (2) gives the equation of motion in the median plane

$$\left(\frac{r'}{\sqrt{r^2+r'^2}}\right)' - \frac{r}{\sqrt{r^2+r'^2}} = -\frac{eH_0}{cp}\frac{r^{k+1}}{r_0^k} f(N\theta) \qquad (9)$$

By putting $\ln \frac{r}{r_1} = q$, (9) becomes

$$\left(\frac{q'}{\sqrt{1+q'^2}}\right)' - \frac{1}{\sqrt{1+q'^2}} = -\frac{eH_0}{cp}\frac{r_1^{k+1}}{r_0^k} e^{(k+1)q} f(N\theta) \qquad (10)$$

where r_1 is chosen as the average radius of the equilibrium orbits so that

$$\int_{-\pi}^{\pi} q \, d(N\theta) = 0$$

From (9), we get

$$(q'' - q'^2 - 1)(1+q'^2)^{-3/2} e^{-(k+1)q} = -\alpha f(N\theta) \qquad (11)$$

where

$$\alpha = \frac{eH_0}{cp}\frac{r_1^{k+1}}{r_0^k} \tag{12}$$

To obtain an approximate solution for q, the left-hand side of (11) is expanded in power series in q and the coefficients of q in Fourier series evaluated by harmonic balance.

By using

$$(q'' - q'^2 - 1)(1+q'^2)^{-3/2} = -1 + q'' + \frac{q'^2}{2}(1-3q'') - \frac{3}{8}q'^4(1-5q'') + \cdots \tag{13}$$

$$e^{-(k+1)q} = 1 - (k+1)q + \frac{(k+1)^2}{2}q^2 - \cdots \tag{14}$$

and

$$q = \sum_j q_j \cos jN\theta \tag{15}$$

the left-hand side of (11) becomes

$$(q'' - q'^2 - 1)(1+q'^2)^{-3/2} e^{-(k+1)q} = \sum c_j \cos jN\theta \tag{16}$$

where (17)

$$C_0 = -1 + \frac{(k+1)N^2}{2} q_1^2 \left\{ 1 + \frac{1}{2(k+1)} - \frac{k+1}{2N^2} \right\}$$

$$+ 2N^2(k+1) q_2^2 \left\{ 1 + \frac{1}{2(k+1)} - \frac{k+1}{8N^2} \right\}$$

$$+ \frac{9}{2} N^2(k+1) q_3^2 \left\{ 1 + \frac{1}{2(k+1)} - \frac{k+1}{18N^2} \right\}$$

$$+ (k+1)^2 q_1^2 q_2 \left\{ \frac{k+1}{6} - \frac{3}{4} N^2 \left(1 + \frac{1}{2(k+1)} \right) \right\}$$

$$+ (k+1)^3 q_1 q_2 q_3 \left\{ \frac{k+1}{4} - \frac{7}{2} N^2 \left(1 + \frac{1}{2(k+1)} \right) \right\} + \cdots$$

$$C_1 = q_1 \left[(k+1) - N^2 + \frac{q_1^2}{8} \left\{ 3N^4 + (k+1)^3 - N^2(k+1) - 3N^2(k+1)^2 \right\} \right.$$

$$+ \frac{q_2^2}{4} \left\{ 12N^4 + (k+1)^3 - 4N^2(k+1) - 9N^2(k+1)^2 \right\}$$

$$+ q_3^2 \left\{ 27N^4 + \frac{(k+1)^3}{6} - 3N^2(k+1) - \frac{5}{2} N^2(k+1)^2 \right\}$$

$$\left. + q_1 q_3 \left\{ \frac{(k+1)^3}{6} - \frac{9}{8} N^4 - \frac{5}{8} N^2(k+1) - \frac{11}{8} N^2(k+1)^2 \right\} \right]$$

$$+ q_2 \left[q_1 \left\{ N^2 - \frac{(k+1)^2}{2} + \frac{5}{2} N^2(k+1) \right\} + q_3 \left\{ 3N^2 - \frac{(k+1)^2}{2} + \frac{13}{2} N^2(k+1) \right\} \right.$$

$$\left. + q_2 q_3 \left\{ \frac{(k+1)^3}{12} - 18N^4 - \frac{N^2(k+1)(2k+5)}{2} \right\} \right]$$

$$C_2 = q_2 \left[(k+1) - 4N^2 + q_1^2 \left\{ 3N^4 + \frac{3}{8}(k+1)^3 - \frac{5}{4} N^2(k+1)^2 + \frac{3}{4} N^2(k+1) \right\} \right.$$

$$+ q_2^2 \left\{ 12N^4 + \frac{(k+1)^2}{12} - N^2(k+1)(k+2) \right\} + q_1 q_3 \left\{ 18N^4 + \frac{(k+1)^3}{6} - N^2(k+1)\frac{(k-5)}{4} \right\}$$

$$\left. + q_3^2 \left\{ \frac{135}{2} N^4 + \frac{(k+1)^3}{6} - \frac{N^2}{4}(k+1)(4k+13) \right\} \right]$$

$$+ q_1 \left[q_1 \left\{ \frac{N^2(k+1)}{2} - \frac{N^2}{4} - \frac{(k+1)^2}{4} \right\} + q_3 \left\{ \frac{3}{2} N^2 - \frac{(k+1)^2}{2} \right\} \right]$$

$$
\begin{aligned}
C_3 = \; & q_3\Big[(k+1) - 9N^2 + q_1^2\Big\{9N^4 + \frac{(k+1)^3}{6} - N^2(k+1) - \frac{5}{2}N^2(k+1)^2\Big\} \\
& + q_2^2\Big\{27N^4 + \frac{(k+1)^3}{6} - \frac{5}{2}N^2(k+1) - \frac{13}{4}N^2(k+1)^2\Big\} \\
& + q_3^2\Big\{\frac{81}{4}N^4 + \frac{(k+1)^3}{12} - \frac{9}{4}N^2(k+1) - \frac{9}{4}N^2(k+1)^2\Big\}\Big] \\
& + q_1\Big[q_2\Big\{-N^2 - \frac{(k+1)^2}{2} + \frac{5}{2}N^2(k+1)\Big\} \\
& + q_1^2\Big\{-\frac{3}{8}N^4 + \frac{(k+1)^3}{24} - \frac{N^2}{8}(k+1)(k+2)\Big\} \\
& + q_2^2\Big\{6N^4 + \frac{(k+1)^3}{12} - \frac{N^2}{2}(k+1)(2k+3)\Big\}\Big]
\end{aligned}
$$

For a pure sinusoidal field ($f(N\theta) = \cos N\theta$), we have

$$
\begin{aligned}
C_0 &= 0 \\
C_1 &= -\alpha \\
C_2 &= 0 \\
C_3 &= 0
\end{aligned}
\qquad (18)
$$

From (17) and (18), by neglecting $\frac{1}{k+1}$ and $\frac{k+1}{N^2}$ compared to unity and also cubic terms of the q's, we obtain

$$
\begin{aligned}
q_1 &\sim \sqrt{\frac{2}{k+1}}\,\frac{1}{N} \\
q_2 &\sim \frac{1}{4N^2} \\
q_3 &\sim \sqrt{\frac{2}{k+1}}\,\frac{1}{N}\Big\{\frac{k+1}{24N^2} - \frac{1}{12(k+1)}\Big\} \\
\alpha &\sim \sqrt{\frac{2}{k+1}}\,N
\end{aligned}
\qquad (19)
$$

Inserting the above values in the higher order terms in (17) and neglecting $\left(\frac{1}{k+1}\right)^2$, $\frac{1}{N^2}$ and $\left(\frac{k+1}{N^2}\right)^2$ compared to unity, the η's are given by

$$\eta_1 \simeq \sqrt{\frac{2}{k+1}}\,\frac{1}{N}\left\{1-\frac{1}{4(k+1)}+\frac{3}{8}\,\frac{k+1}{N^2}\right\} \tag{20}$$

$$\eta_2 \simeq \frac{1}{4N^2}\left\{1+\frac{1}{k+1}+\frac{3}{8}\,\frac{k+1}{N^2}\right\}$$

$$\eta_3 \simeq \sqrt{\frac{2}{k+1}}\,\frac{1}{N}\left\{\frac{k+1}{24N^2}-\frac{1}{12(k+1)}\right\}\left\{1-\frac{1}{4(k+1)}+\frac{3}{8}\,\frac{k+1}{N^2}\right\}$$

$$\alpha \simeq \sqrt{\frac{2}{k+1}}\,N\left\{1-\frac{1}{k+1}-\frac{k+1}{2N^2}\right\}$$

The circumference factor C is given by

$$C \simeq \alpha\left(1+\eta_1+\eta_2+\eta_3\right)^{k+1} \tag{21}$$

$$\simeq \sqrt{\frac{2}{k+1}}\,N\left\{1+\frac{k+1}{N^2}\right\}+2$$

The above estimate of the η's and α agrees well with the results obtained from the digital computer. Since the betatron oscillations are a more sensitive check on the orbit estimates, direct comparisons of η's and α are not shown.

The circumference factors obtained by (21) are compared with the computer results in Table 1.

TABLE I - Circumference Factor

N	k+1	C anal	C digital
64	200	8.7	8.6
64	160	9.4	9.3
64	120	10.4	10.4
24	25	8.5	8.8
24	18	9.5	9.8
18	13	8.4	8.8
18	12	8.7	9.1
18	10	9.2	9.6

BETATRON OSCILLATION

To obtain the equations for linear betatron oscillations around the oribts, the "soft-edge equations"[6] are used, because the large scalloping of the orbits makes the method of expansion[7] used for the spiral sector machine troublesome.

In the soft-edge equations,[8]

$$\frac{d^2x}{ds^2} + \left[\frac{F^2(s)}{\rho_0^2} + \frac{n_0}{\rho_0^2} F(s) \frac{r_0}{r_e} + \frac{1}{\rho_0} \frac{dF}{ds} \tan\phi \right] x = 0$$

$$\frac{d^2z}{ds^2} - \left[\frac{n_0}{\rho_0^2} F(s) \frac{r_0}{r_e} + \frac{1}{\rho_0} \frac{dF}{ds} \tan\phi \right] z = 0 \qquad (22)$$

---

(6) F.T. Cole et al R.S.I. 28, 403 (1957)

(7) F.T. Cole, MURA-F.T.C-3

(8) The same notations in reference [6] are used.

we have

$$F(s) = \left(\frac{r_e}{r_0}\right)^k f(N\theta)$$

$$\ln \frac{r_e}{r_1} = \sum g_j \cos jN\theta \equiv h(N\theta) \tag{23}$$

for our case.

(22) and (23) give

$$\frac{d^2x}{ds^2} + \frac{1}{r_1^2}\left[\alpha^2 e^{2kh(N\theta)} f^2(N\theta) + \alpha e^{(k-1)h(N\theta)} \{kf(N\theta) - h'(N\theta) f'(N\theta)\}(1+h'^2(N\theta))^{-1/2}\right] x = 0 \tag{24}$$

$$\frac{d^2z}{ds^2} - \frac{1}{r_1^2}\left[\alpha e^{(k-1)h(N\theta)} \{kf(N\theta) - h'(N\theta) f'(N\theta)\}(1+h'^2(N\theta))^{-1/2}\right] z = 0$$

$$s = r_1 \int e^{\frac{h(N\theta)}{\sqrt{1+h'^2(N\theta)}}} d\theta \tag{25}$$

By using (23) and (20), s is given by

$$s - s_0 \simeq r_1 \left[\theta\left(1 + \frac{1}{2(k+1)}\right) + \frac{3}{2N^2}\sqrt{\frac{2}{k+1}} \sin N\theta + \cdots\right] \tag{26}$$

Defining $\textcircled{H}$ by

$$\textcircled{H} = \frac{\delta - \delta_0}{r_1\left(1+\frac{1}{2(k+1)}\right)} \tag{27}$$

and assuming

$$\textcircled{H} \simeq \theta$$

the equations (24) become

$$\frac{d^2x}{d\textcircled{H}^2} + \left(1+\frac{1}{2(k+1)}\right)^2 \Big[\alpha^2 e^{2k h(N\textcircled{H})} f(N\textcircled{H}) + \alpha e^{(k-1)h(N\textcircled{H})} \{k f(N\textcircled{H}) - h'(N\textcircled{H}) f'(N\textcircled{H})\}(1+h'^2(N\textcircled{H}))^{-\frac{1}{2}} \Big] x = 0 \tag{28}$$

$$\frac{d^2z}{d\textcircled{H}^2} - \left(1+\frac{1}{2(k+1)}\right)^2 \Big[\alpha e^{(k-1)h(N\textcircled{H})} \{k f(N\textcircled{H}) - h'(N\textcircled{H}) f'(N\textcircled{H})\}(1+h'^2(N\textcircled{H}))^{-\frac{1}{2}} \Big] z = 0$$

All terms depending on $\textcircled{H}$ in the above equations are evaluated in Fourier series form

$$e^{(k-1)h(N\textcircled{H})}(1+h'^2(N\textcircled{H}))^{-\frac{1}{2}} = \sum C_j \cos jN\textcircled{H}$$

$$k f(N\textcircled{H}) - h'(N\textcircled{H}) f'(N\textcircled{H}) = \sum D_j \cos jN\textcircled{H} \tag{29}$$

$$e^{2kh(N\textcircled{H})} f^2(N\textcircled{H}) = \sum E_j \cos jN\textcircled{H}$$

where

$$C_0 \doteq 1 + \frac{q_1^2}{4}\left\{(k-1)^2 - N^2\right\} + \frac{q_2^2}{4}\left\{(k-1)^2 - 4N^2\right\}$$

$$C_1 \doteq q_1\left[(k-1) + \frac{N^2}{4}(k-1)\left\{-\frac{q_1^2}{2} - 4q_2^2 - 12q_3^2 - \frac{5}{2}q_1q_3\right\}\right]$$

$$+ q_2\left[q_1\left\{-N^2 + \frac{(k-1)^2}{2}\right\} + q_3\left\{-3N^2 + \frac{(k-1)^2}{2}\right\} - \frac{3}{2}(k-1)N^2 q_2 q_3\right]$$

$$C_2 \doteq (k-1)q_2 + \frac{q_1^2}{4}\left\{N^2 + (k-1)^2\right\} + \frac{q_1q_3}{2}\left\{(k-1) - 3N^2\right\}$$

$$+ (k-1)N^2\left\{-\frac{q_1^2 q_2}{4} + q_2^3 - 2q_1q_2q_3 - \frac{11}{4}q_2q_3^2\right\}$$

$$C_3 \doteq (k-1)q_3 + q_1q_2\left\{\frac{(k-1)^2}{2} + N^2\right\} + (k-1)N^2\left\{-q_1^2q_3 - \frac{q_2^2q_3}{2} + \frac{9}{4}q_3^2 + \frac{q_1^3}{8} - \frac{q_1q_2^2}{2}\right\}$$

$$D_0 \doteq -\frac{q_1}{2}N^2$$

$$D_1 \doteq k - q_2N^2$$

$$D_2 \doteq \frac{N^2}{2}(q_1 - 9q_3)$$

$$D_3 \doteq N^2 q_2$$

$$E_0 \doteq \frac{1}{2} + \frac{kq_2}{2} + \frac{k^2}{2}\left\{\frac{3}{2}q_1^2 + q_2^2 + q_3^2 + q_1q_3\right\}$$

$$E_1 \doteq \frac{3}{2}kq_1 + \frac{kq_3}{2} + 2k^2q_1q_2 + \frac{3}{2}k^2q_2q_3$$

$$E_2 \doteq \frac{1}{2} + kq_2 + k^2\left\{q_1^2 + q_1q_3 + \frac{q_2^2}{2} + \frac{q_3^2}{2}\right\}$$

$$E_3 \doteq k(q_1 + q_3) + k^2(2q_1q_2 + q_2q_3)$$

By using (20) in (29), we obtain

$$C_0 \simeq 1 - \frac{1}{2(k+1)} + \frac{k+1}{2N^2}$$

$$C_1 \simeq \frac{\sqrt{2(k+1)}}{N}\left[1 - \frac{11}{4(k+1)} + \frac{k+1}{2N^2}\right]$$

$$C_2 \simeq \frac{1}{2(k+1)} + \frac{3(k+1)}{4N^2}$$

$$C_3 \simeq \frac{\sqrt{2(k+1)}}{N}\left[\frac{5}{12(k+1)} + \frac{k+1}{6N^2}\right]\left[1 - \frac{9}{4(k+1)} + \frac{3}{8}\frac{(k+1)}{N^2}\right]$$

$$D_0 \simeq -\frac{N}{\sqrt{2(k+1)}}\left[1 - \frac{1}{4(k+1)} + \frac{3(k+1)}{8N^2}\right]$$

$$D_1 \simeq (k+1)\left\{1 - \frac{5}{4(k+1)}\right\} \qquad (30)$$

$$D_2 \simeq \frac{N}{\sqrt{2(k+1)}}\left\{1 + \frac{1}{4}\frac{k+1}{N^2}\right\}$$

$$D_3 \simeq \frac{1}{4}\left\{1 + \frac{1}{k+1} + \frac{3}{8}\frac{k+1}{N^2}\right\}$$

$$E_0 \simeq \frac{1}{2} + \frac{13}{8}\frac{k+1}{N^2}$$

$$E_1 \simeq \frac{\sqrt{2(k+1)}}{N}\left\{1 - \frac{23}{18(k+1)} + \frac{13}{18}\frac{k+1}{N^2}\right\}$$

$$E_2 \simeq \frac{1}{2}\left\{1 + \frac{9}{2}\frac{k+1}{N^2}\right\}$$

$$E_3 \simeq \frac{\sqrt{2(k+1)}}{N}\left\{1 - \frac{4}{3(k+1)} + \frac{11}{12}\frac{k+1}{N^2}\right\}$$

Using above values, the equations (28) become

$$\frac{d^2x}{d\theta^2} + \left[A_{x0} + A_{x1}\cos N\theta + A_{x2}\cos 2N\theta + A_{x3}\cos 3N\theta \right] x = 0 \qquad (31)$$

$$\frac{d^2z}{d\theta^2} + \left[A_{z0} + A_{z1}\cos N\theta + A_{z2}\cos 2N\theta + A_{z3}\cos 3N\theta \right] z = 0$$

where

$$A_{x0} \simeq (k+1)\left\{1 - \frac{7}{4(k+1)}\right\}$$

$$A_{x1} \simeq \sqrt{2(k+1)}\, N \left\{1 + \frac{3}{8}\frac{k+1}{N^2}\right\}$$

$$A_{x2} \simeq (k+1)\left\{1 - \frac{1}{3(k+1)} + \frac{k+1}{6N^2}\right\} + \frac{2N^2}{k+1}\left\{1 - \frac{1}{2(k+1)}\right\}$$

$$A_{x3} \simeq \sqrt{\frac{2}{k+1}}\, N\left\{2 - \frac{49}{6(k+1)} - \frac{25}{48}\frac{k+1}{N^2}\right\} + \frac{3}{8}\frac{\sqrt{2(k+1)}\,(k+1)}{N}$$

$$A_{z0} \simeq -(k+1)\left(1 - \frac{4}{k+1}\right) + \frac{N^2}{k+1}\left(1 - \frac{1}{k+1}\right)$$

$$A_{z1} \simeq -\sqrt{2(k+1)}\, N\left\{1 - \frac{2}{k+1} + \frac{3}{8}\frac{k+1}{N^2}\right\}$$

$$A_{z2} \simeq -(k+1)\left\{1 - \frac{23}{6(k+1)} + \frac{k+1}{6N^2}\right\} - \frac{N^2}{k+1}\left\{1 - \frac{1}{k+1}\right\}$$

$$A_{z3} \simeq -\sqrt{\frac{2}{k+1}}\, N\left\{1 - \frac{2}{k+1} - \frac{17}{48}\frac{k+1}{N^2}\right\} - \frac{3}{8}\frac{\sqrt{2(k+1)}}{N}(k+1)$$

To calculate the betatron oscillation frequencies from the equations (31), Vogt-Nilsen's formulas[9] are used.

$$\cos\sigma_x \simeq \cos\frac{2\pi\sqrt{A_{x0}}}{N} - \frac{\pi}{2N}\frac{\sin\frac{2\pi\sqrt{A_{x0}}}{N}}{\sqrt{A_{x0}}}\left[\frac{A_{x1}^2}{N^2-4A_{x0}} + \frac{A_{x2}^2}{4N^2-4A_{x0}} + \frac{3A_{x1}^2A_{x2}}{(N^2-4A_{x0})(4N^2-4A_{x0})}\right]$$

$$\cos\sigma_z \simeq \cosh\frac{2\pi\sqrt{-A_{z0}}}{N} - \frac{\pi}{2N}\frac{\sinh\frac{2\pi\sqrt{-A_{z0}}}{N}}{\sqrt{-A_{z0}}}\left[\frac{A_{x1}^2}{N^2-4A_{z0}} + \frac{A_{z2}^2}{4N^2-4A_{z0}} + \frac{3A_{z1}^2A_{z2}}{(N^2-4A_{z0})(4N^2-4A_{z0})}\right] \qquad (32)$$

The calculated σ_x for various machine parameters are shown in Table 2 compared with the results obtained by digital computation.

---

(9) N. Vogt-Nilsen, MURA-118

TABLE - 2

N	k+1	$\frac{\sigma_x}{\pi}$ anal	$\frac{\sigma_x}{\pi}$ digit	$\frac{\sigma_z}{\pi}$ anal	$\frac{\sigma_z}{\pi}$ digit
64	200	.765	.764	.134	.109
	160	.639	.641	.158	.143
	120	.529	.531	.186	.179
24	25	.699	.743	.422	.412
	18	.563	.595	.485	.487
18	12	.644	.710	.596	.605
	10	.580	.636	.641	.666

In large N machines, the σ_x's agree well and the apparent larger errors in σ_z's are due to the fact that a small error in cos σ causes a large error in σ because σ is small. For small N machine correction terms of order $\frac{1}{k+1}$ get larger and make agreement poorer.

The smooth approximation may be used for estimating σ roughly. The equations (31) are approximately

$$\frac{d^2x}{d\theta^2} + \left[(k+1) + \sqrt{2(k+1)}\, N\cos N\theta + \left\{k+1 + \frac{2N^2}{k+1}\right\}\cos 2N\theta\right] x \simeq 0$$

(33)

$$\frac{d^2z}{d\theta^2} + \left[-(k+1) + \frac{N^2}{k+1} - \sqrt{2(k+1)}\, N\cos N\theta - \left\{k+1 + \frac{N^2}{k+1}\right\}\cos 2N\theta\right] z \simeq 0$$

The σ_j are given by

$$\frac{\sigma_x}{\pi} \sim \frac{2\sqrt{2(k+1)}}{N}$$

$$\frac{\sigma_z}{\pi} \sim \frac{2}{\sqrt{k+1}} \qquad (34)$$

By multiplying (34) each other, we obtain

$$\left(\frac{\sigma_x}{\pi}\right)\cdot\left(\frac{\sigma_z}{\pi}\right) \sim \frac{4\sqrt{2}}{N} \qquad (35)$$

For a working point in the first stable region, (35) should be less than unity and it indicates that there is a lower limit on N to obtain stable motions.

In Fig. 1 σ_x is plotted against σ_z .

From (21) and (34), the circumference factor C is roughly given by

$$C \sim \frac{4}{\left(\frac{\sigma_x}{\pi}\right)} + 2 \qquad (36)$$

and this shows the minimum circumference factor for a sinusoidal field is ~ 6 For a rectangular field this figure would be reduced by a factor $\sqrt{2}$.

Since we would rather use σ_x between $(2/3)\pi$ and π to make the circumference factor as small as possible, the smooth approximation always underestimates σ_x . If we plot σ_x against $\frac{k+1}{N^2}$, it looks more like a straight line than the parabola expected by the smooth approximation.

Furthermore, if σ_x is plotted against $\frac{k+3.5}{N^2}$ all points lie approximately on a straight line independent of N , as shown in Fig. 2. So we have a handy empirical formula for σ_x

$$\frac{\sigma_x}{\pi} \sim 11.9\left(\frac{k+25}{N^2}\right) + 0.175 \qquad (37)$$

Similarly σ_z is plotted against $\frac{2}{\sqrt{k+1}}$ which the smooth approximation predicts in Fig. 3 and we obtain a handy formula for σ_z

$$\frac{\sigma_z}{\pi} \sim 1.105\left(\frac{2}{\sqrt{k+1}} - 0.03\right) \qquad (38)$$

The σ_x obtained by (37) and (38) are compared with the computer results in Table 3 and Table 4.

TABLE - 3

N	k+1	$\frac{\sigma_x}{\pi}$ emp. form.	$\frac{\sigma_x}{\pi}$ digit
64	200	.763	.764
	160	.646	.641
	120	.531	.531
36	40	.565	.563
24	25	.743	.743
	18	.599	.595
18	13	.744	.750
	12	.708	.710
	10	.634	.636
16	9.5	.733	.741

TABLE - 4

N	k+1	$\frac{\sigma_z}{\pi}$ emp. Form	$\frac{\sigma_z}{\pi}$ digit
18	13	.580	.580
	12	.605	.605
	10	.666	.666
24	25	.409	.412
	18	.488	.488
64	200	.123	.109
	160	.142	.143
	120	.169	.179

HIGHER HARMONICS

The magnetic fields in actual machines contain higher harmonics which are usually smaller than those of rectangular fields. The effects of the j-th harmonic on the orbits and the gradient focusing are reduced by a factor $\frac{1}{j^2}$ and very little change in σ_x is expected by adding harmonics. Table 5 shows the σ_x is hardly change by adding third harmonics.

TABLE - 5 Harmonics and

N	k+1	σ_x/π Sinusoidal	Third harmonic content	σ_r/π
18	12	.71	-25%	.71
18	10	.64	-25%	.64
24	25	.74	-30%	.74
24	18	.60	-33%	.60
64	200	.76	-33%	.75

The circumference factor is reduced by adding harmonics, since the orbits are almost unaffected and the peak field is reduced. When the harmonic content is smaller than that of a rectangular field the circumference factor is approximately given by

$$C \sim C_{sin} \frac{\sum f_{2j+1}}{f_1} \tag{39}$$

where C sin : circumference factor of sinusoidal field and the field is assumed to have the form (8).

According to the smooth approximation, σ_z is given by

$$\left(\frac{\sigma_z}{\pi}\right)^2 \sim \left(\frac{\sigma_z}{\pi}\right)^2_{sin} F^2 \tag{40}$$

where

$\left(\frac{\sigma_z}{\pi}\right)_{sin}$ $\left(\frac{\sigma_z}{\pi}\right)$ for sinusoidal field

$$F^2 = \frac{\sum f_{2j+1}^2}{f_1^2}$$

$\left(\frac{\nu_z}{\pi}\right)^2 \Big/ \left(\frac{\nu_z}{\pi}\right)^2_{sin}$ is plotted against F^2 in Fig. 4. It is clear in the figure that the increment of ν_z is more than that given by the smooth approximation. ν_z is given very roughly by

$$\left(\frac{\nu_z}{\pi}\right)^2 \sim \left(\frac{\nu_z}{\pi}\right)^2_{sin} \left[F^2 + \sqrt{F^2 - 1} \times 0.16 \right] \qquad (41)$$

SPIRALLING

In a large N machine, say $N > 100$, spiralling might be necessary to obtain a comfortable ν_z. The orbits and the radial tunes change very little. The smooth approximation formula for the axial tune is given by

$$\left(\frac{\nu_z}{\pi}\right)^2 \sim \frac{4F^2}{k+1} \left[1 + \frac{2}{N^2 W^2} \right] \qquad (42)$$

Stability limits would be decreased by spiralling due to the additional non-linearity of the fields.

STABILITY LIMITS

According to G. Parzen's[10] formula for stability limit due to non-linear resonance lines, there are no remarkable differences from the ordinary radial sector machine, except that the Walkinshaw's line ($\nu_x - 2\nu_z = 0$) is almost forbidden in this machine.[10]

---

(10) G. Parzen, MURA-300

The stability limit amplitude of the radial motion due to the $\sigma_x = (2/3)\pi$ resonance line is given by

$$A = \frac{2}{MN^2} \left| \left(\frac{\sigma_x}{2\pi}\right)^2 - \left(\frac{1}{3}\right)^2 \right| \qquad (43)$$

where

$$M = \frac{\alpha}{4} \frac{(k+1)^2}{N^4} \left(1 + \frac{28(k+1)}{N^2}\right)$$

The above formula is compared with the results from the computer in the following table.

N	k+1	A anal	A digit
20	16.1	1.9×10^{-2}	1.3×10^{-2}
36	58	5.0×10^{-3}	3.9×10^{-3}

For the sum resonance line, $\sigma_x + 2\sigma_z = 2\pi$ the stability limit amplitudes are given by[10]

$$A = \frac{1}{MN^2} \left| \left(\frac{\sigma_{z0}}{2\pi}\right)^2 - \left(\frac{\sigma_z}{2\pi}\right)^2 \right|$$

$$B = \frac{1}{MN^2} \left\{ 2 \left| \left(\frac{\sigma_{x0}}{2\pi}\right)^2 - \left(\frac{\sigma_x}{2\pi}\right)^2 \right| \left| \left(\frac{\sigma_{z0}}{2\pi}\right)^2 - \left(\frac{\sigma_z}{\pi}\right)^2 \right| \right\}^{1/2} \qquad (44)$$

where

$$M = \frac{\alpha}{4} \frac{(k+1)^2}{N^4}$$

A and B depend on the tunes σ_x and σ_z at the stability boundary to which σ_{x0} and σ_{z0} are driven. It takes long series of computer runs to obtain

A and B as a function of initial values of x and z. This survey has not been done. However, few values of A and B obtained so far indicate fair agreements with (44).

TWO-BEAM - ONE-BEAM TUNING

Since the symmetric machine is a special case of the radial sector FFAG machine, the machine can be used as a one-beam radial sector machine by changing the magnitude of the magnetic fields in the positive and the negative magnets.

If $f(N\theta)$ is given by

$$f(N\theta) = \epsilon + \cos N\theta \tag{45}$$

the smooth approximation gives

$$\left(\frac{\nu_x}{\pi}\right)^2 \sim \frac{4(k+1)}{N^2}\left\{1 + \frac{\alpha'^2(k+1)}{2N^2}\right\} \tag{46}$$

$$\left(\frac{\nu_z}{\pi}\right)^2 \sim 4\left\{\frac{\alpha'^2}{2N^2} + \frac{\alpha'^2(k+1)^2}{2N^4} - \frac{k+1}{N^2}\right\}$$

where [11] $\alpha' = \frac{N^2}{k+1}\left[\sqrt{\frac{\epsilon^2}{4} + \frac{2(k+1)}{N^2}} - \frac{\epsilon}{2}\right]$

---

(11) α' is $b/2h_1$ in G. Parzen's notation in his report MURA-273

By eliminating α' in (46), we obtain

$$\left(\frac{\nu_x}{\pi}\right)^2\left[1+\frac{N^2}{(k+1)^2}\right]-\left(\frac{\nu_z}{\pi}\right)^2 \sim \frac{4}{k+1}+\frac{8(k+1)}{N^2} \qquad (47)$$

This shows the working points move along a hyperbola by changing the magnets excitation. It must be noted that this is the smooth approximation result and shows only rough behavior of the working points, especially for high σ's.

EXAMPLES OF DESIGN PARAMETERS

In the following typical sets of parameters for rather small size machines are discussed.

Unfortunately direct Forocyl-Formesh calculation can not be used with vanishing average value of the magnetic field. The calculations are done as follows. In the magnet configurations of Forocyl agenda, a finite value of potential on the positive (negative) magnet and zero on the negative (positive) magnet are given. The configurations have the symmetry around the centers of the positive magnets and also around that of the negative magnets. By picking up only odd Fourier coefficients of the median plane fields in the output of Forocyl, we have the median plane field when both positive and negative magnets are energized. This field can be used to calculate dynamics by the Well Tempered Five program. (The alternative is to feed this field in Tempermesh and use Formesh for dynamics)[12] It must be noted that all field coefficients are normalized to $f_1 = 1$ and then multiplied by α to run dynamics to keep x within the range of the program.

(12) This procedure is being used for New Model by A. Sessler and F.T. Cole.

N for small size (electron) machine might range $14 \sim 24$ considering the magnet gaps and straight sections. In this range $N = 18$ must be discarded because the working points stay always too close to the line $\sigma_x + 2\sigma_z = 2\pi$ which is an essential and dangerous line.

EXAMPLE 1.

$N = 20$ $\quad k = 15.1$

The configuration of magnets is shown in Fig. 5.

Fourier components of median plane fields

1st	1.000 000
3rd	- 0.228407
5th	0.054433
7th	0.004272
9th	- 0.017548
11th	0.014469
13th	- 0.008186

Circumference factor 7.2

$\sigma_x/\pi \simeq 0.727$ $\quad \sigma_z/\pi \simeq 0.547$

Phase plots of x and z motion are shown in Fig. 8 and Fig. 9.

Radius	at injection	200 cm
	at output	275 cm
Energy	at injection	100 Kev
	at output	50 Mev
H_{max}		4300 gausses

EXAMPLE 2.

$N = 16$ $\quad k = 8.5$

The magnet configuration is shown in Fig. 6.

Fourier components of the median plane fields

1st	1.000 000
3rd	- 0.228394
5th	0.054391
7th	0.004341
9th	- 0.017617
11th	0.014520
13th	- 0.008215

Circumference factor 7.2

$\sigma_r/\pi \simeq 0.746$ $\sigma_z/\pi \simeq 0.739$

Radius at injection 200 cm

at output 340 cm

Energy at injection 100 Kev

at output 50 Mev

H_{max} 3500 gausses

EXAMPLE 3.

$N = 36$ $k = 57$

The magnet configuration is shown in Fig. 7.

Fourier components of the median plane fields

1st	1.000 000
3rd	- 0.264663
5th	0.092525
7th	- 0.017268
9th	- 0.015356
11th	0.024919
13th	- 0.022792
15th	0.016176

$\sigma_r/\pi \simeq .718$ $\sigma_z/\pi \simeq .275$

Circumference factor 7.07

Radius	at injection	890 cm
	at output	1000 cm
Energy	at injection	100 Kev
	at output	300 Mev
H_{max}		7000 gausses

OTHER PROBLEMS

Since the machine is different from the ordinary FFAG accelerator only in the particle dynamics, the problems such as, acceleration, injection, stacking, space charge effects and so on, are the same as in the ordinary FFAG machine. The discussions of these problems can be found in numerous MURA reports.

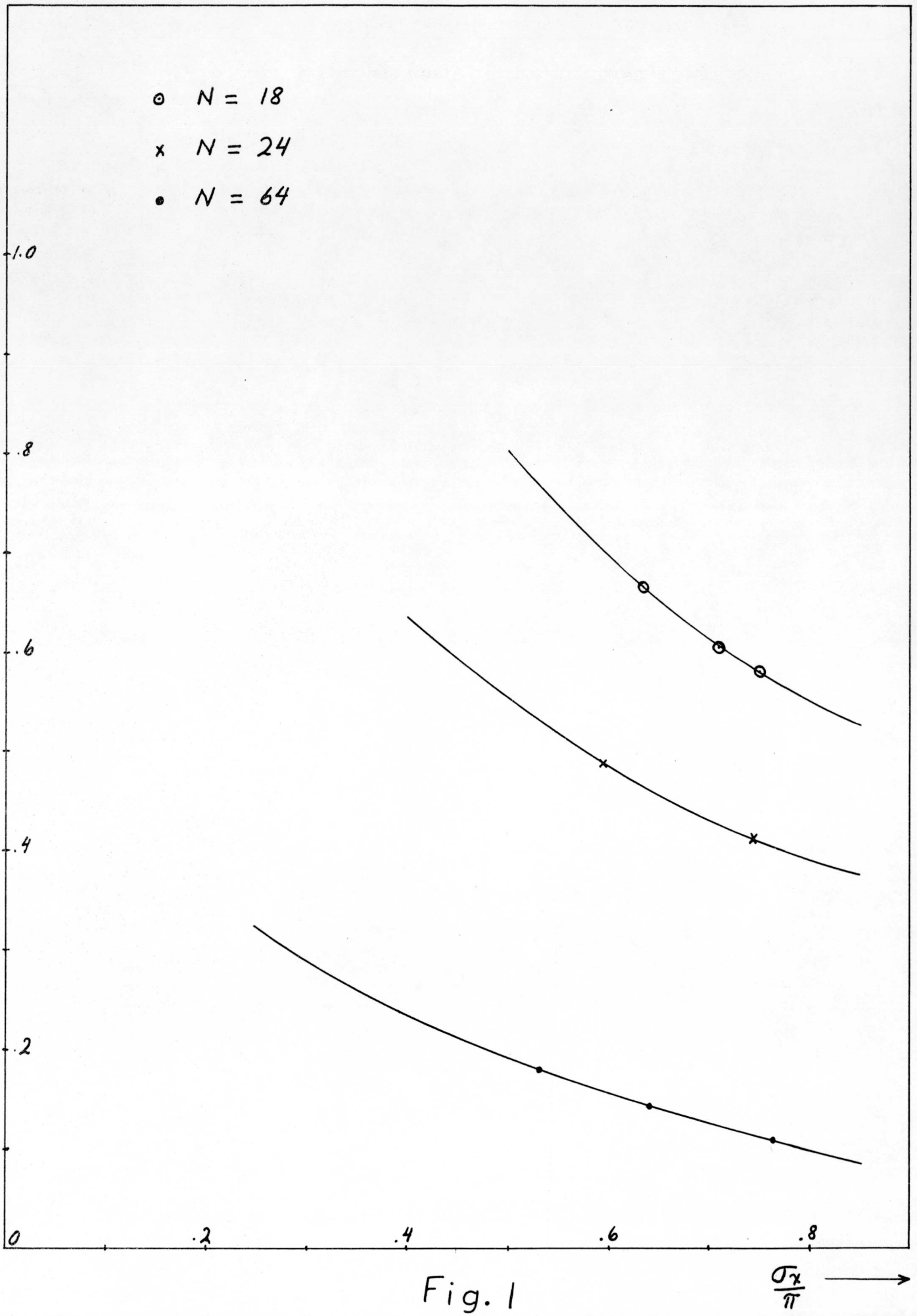

Fig. 1

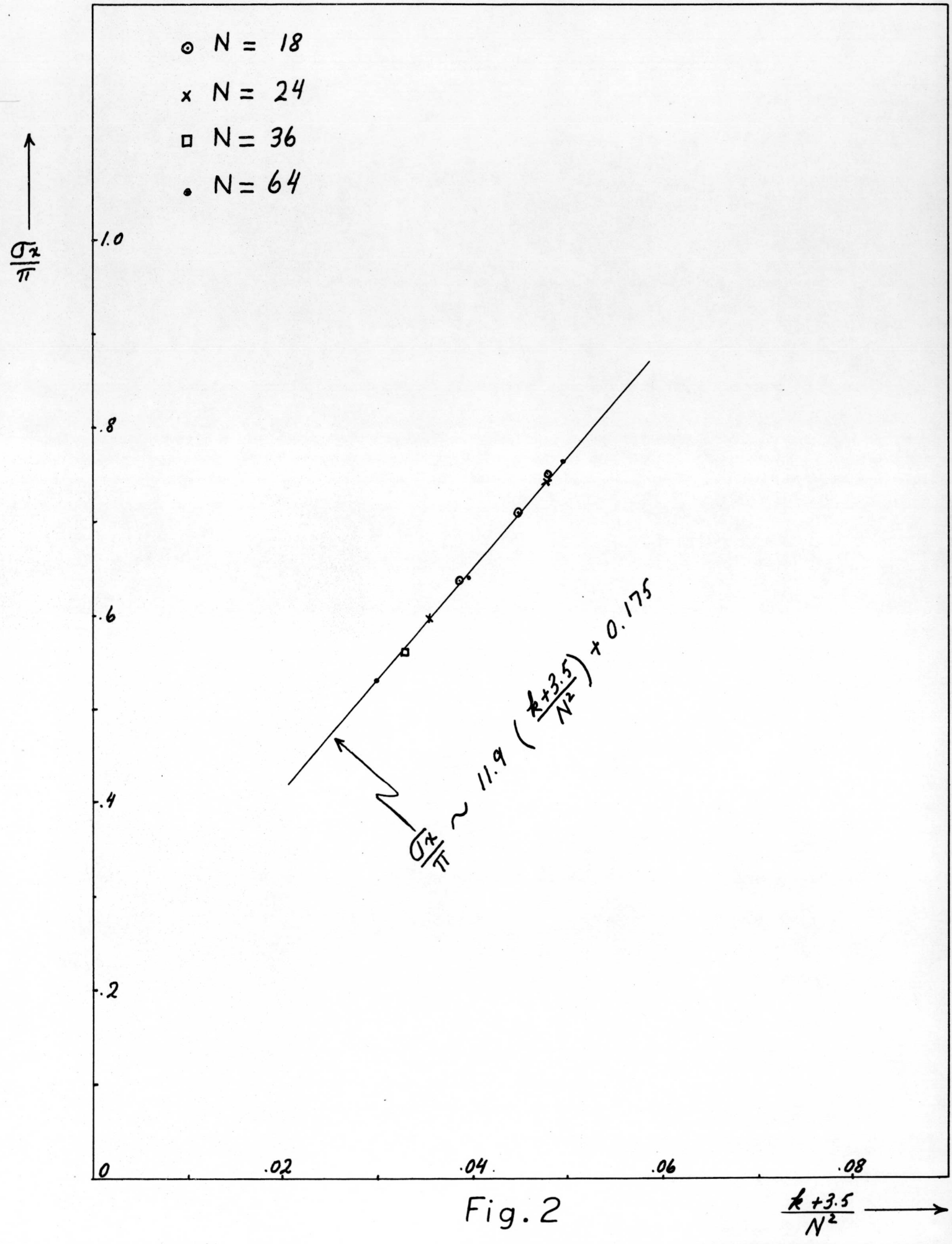
⊙ N = 18
× N = 24
□ N = 36
• N = 64
$\frac{\sigma_x}{\pi}$
1.0
.8
.6
.4
.2
0
.02
.04
.06
.08
$\frac{\sigma_x}{\pi} \sim 11.9 \left(\frac{k+3.5}{N^2}\right) + 0.175$
$\frac{k+3.5}{N^2}$

Fig. 2

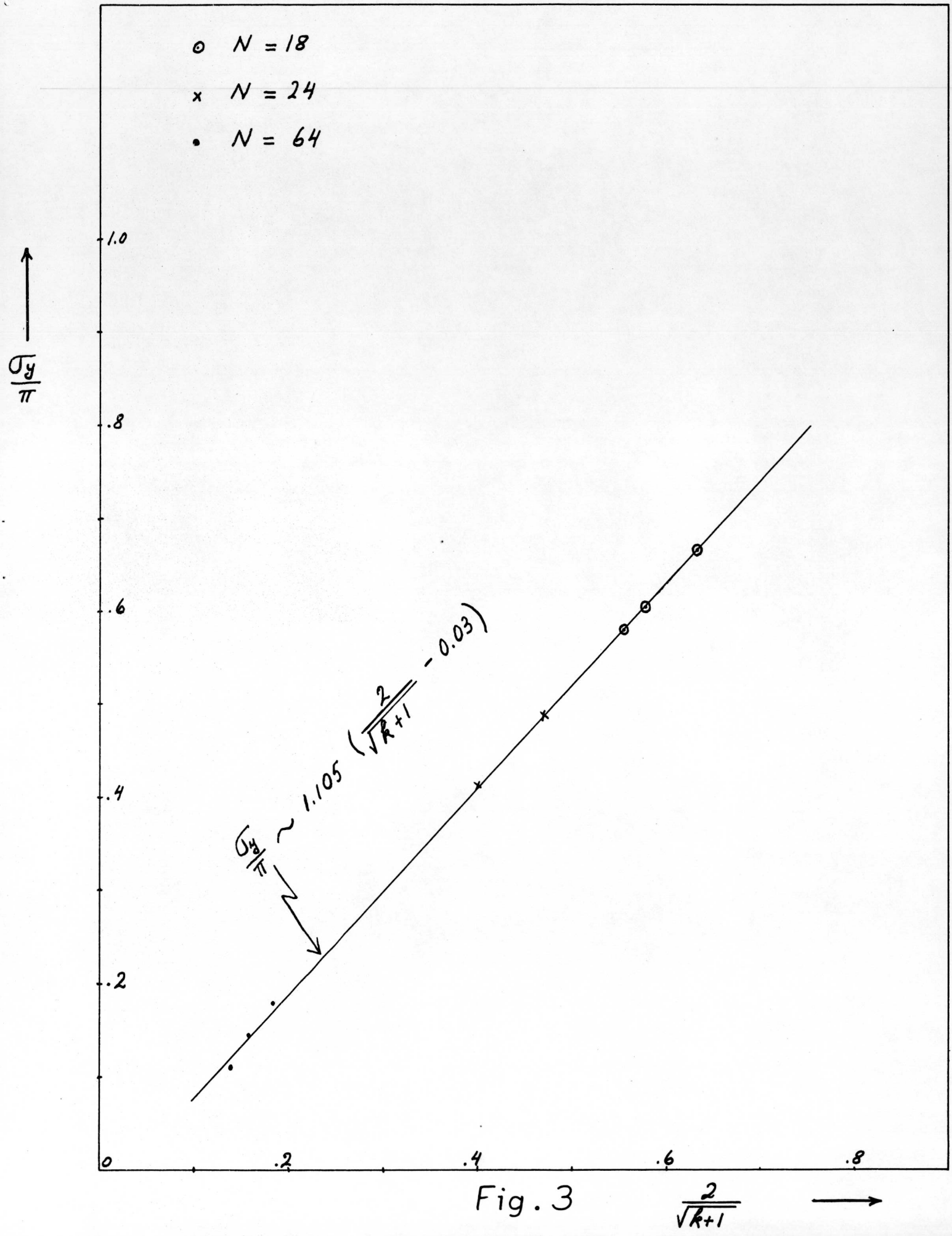
o N = 18
x N = 24
• N = 64
$\frac{\sigma_y}{\pi}$
1.0
.8
.6
.4
.2
0
.2
.4
.6
.8
$\frac{\sigma_y}{\pi} \sim 1.105 \left(\frac{2}{\sqrt{k+1}} - 0.03\right)$
$\frac{2}{\sqrt{k+1}}$

Fig. 3

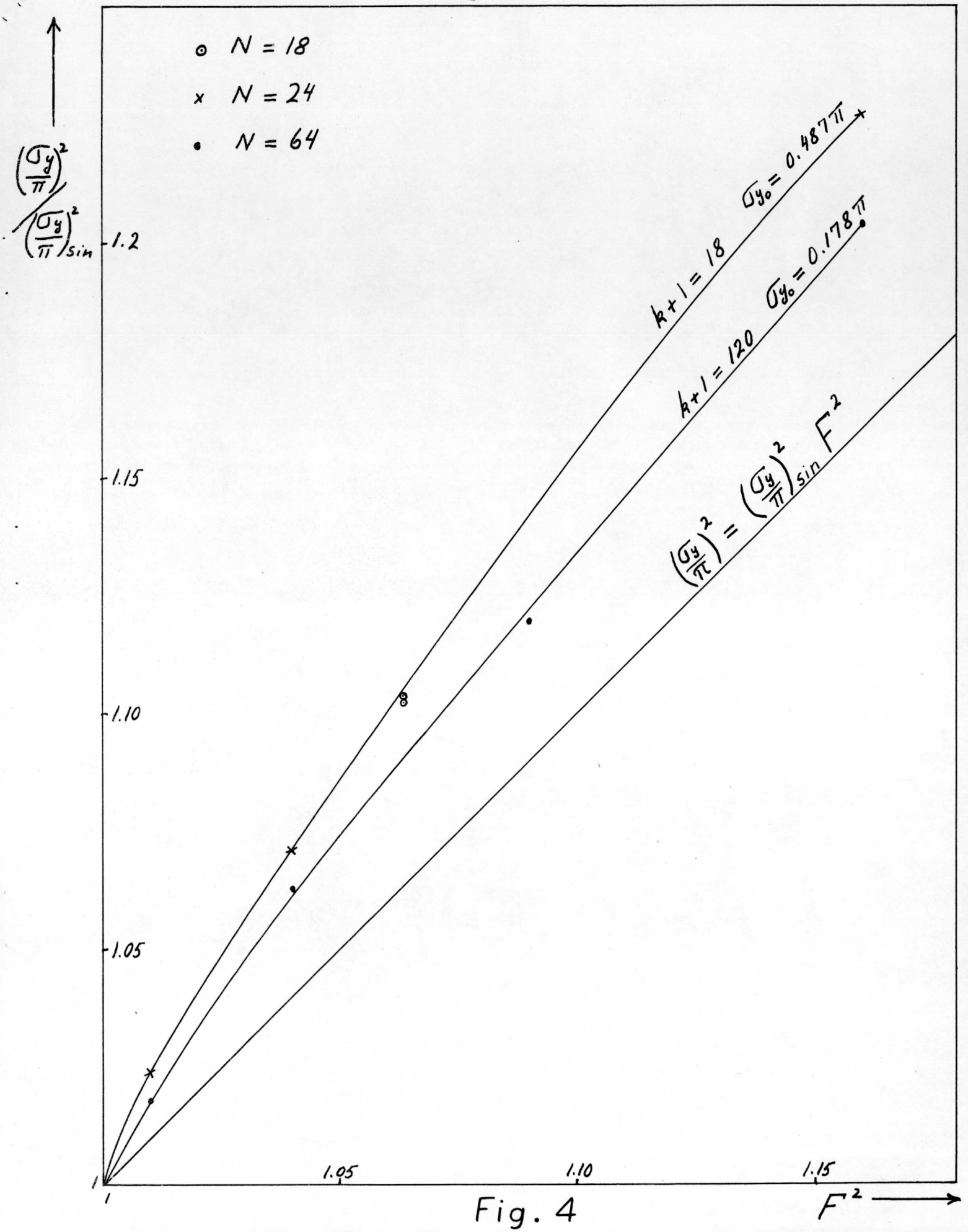
N = 18
N = 24
N = 64
$\left(\frac{\sigma_y}{\pi}\right)^2 / \left(\frac{\sigma_y}{\pi}\right)^2_{sin}$
1.2
1.15
1.10
1.05
1
1.05
1.10
1.15
F^2
$k+1 = 18$ $\sigma_{y_0} = 0.487\pi$
$k+1 = 120$ $\sigma_{y_0} = 0.178\pi$
$\left(\frac{\sigma_y}{\pi}\right)^2 = \left(\frac{\sigma_y}{\pi}\right)^2_{sin} F^2$

Fig. 4

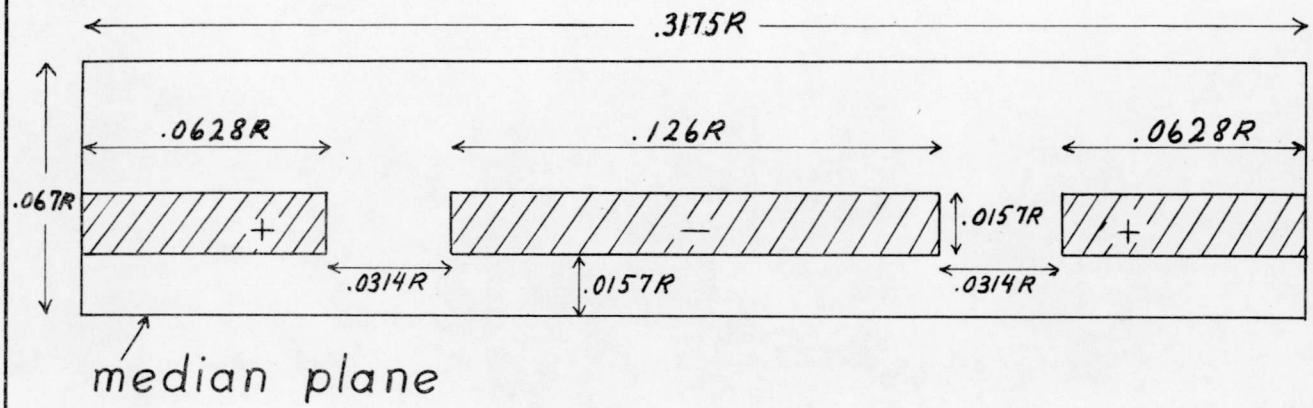

Fig. 5

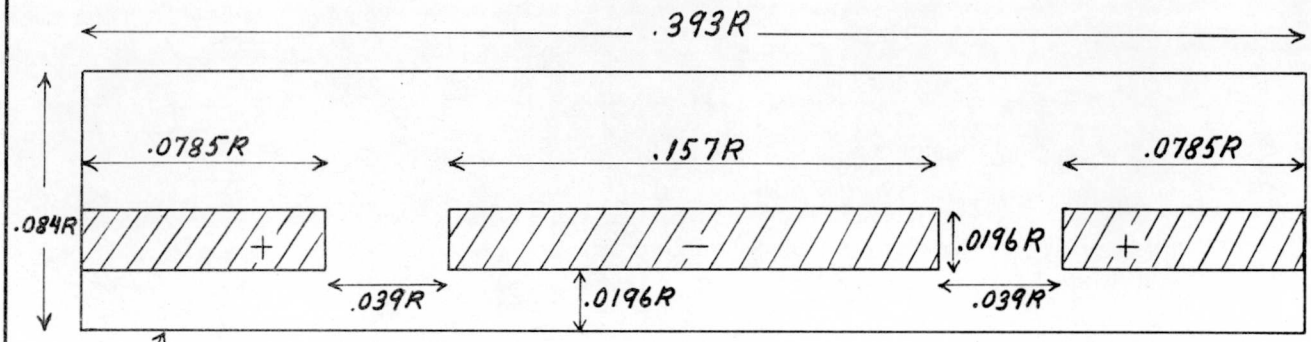

Fig. 6

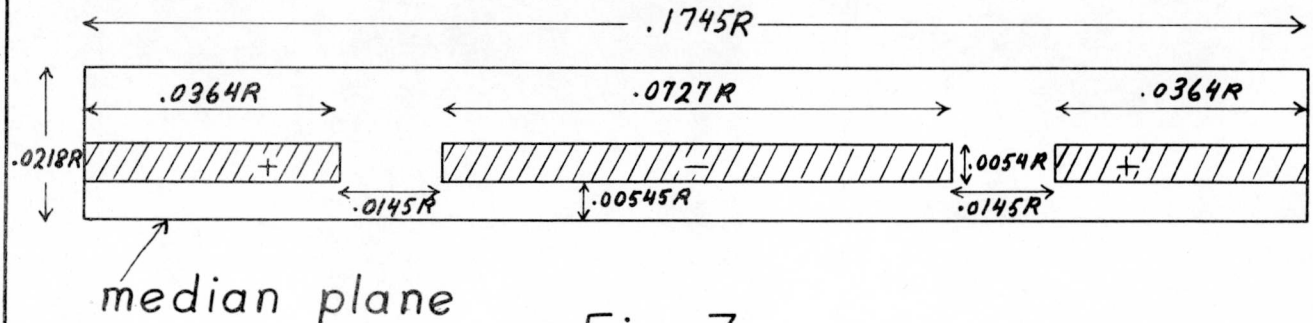

Fig. 7

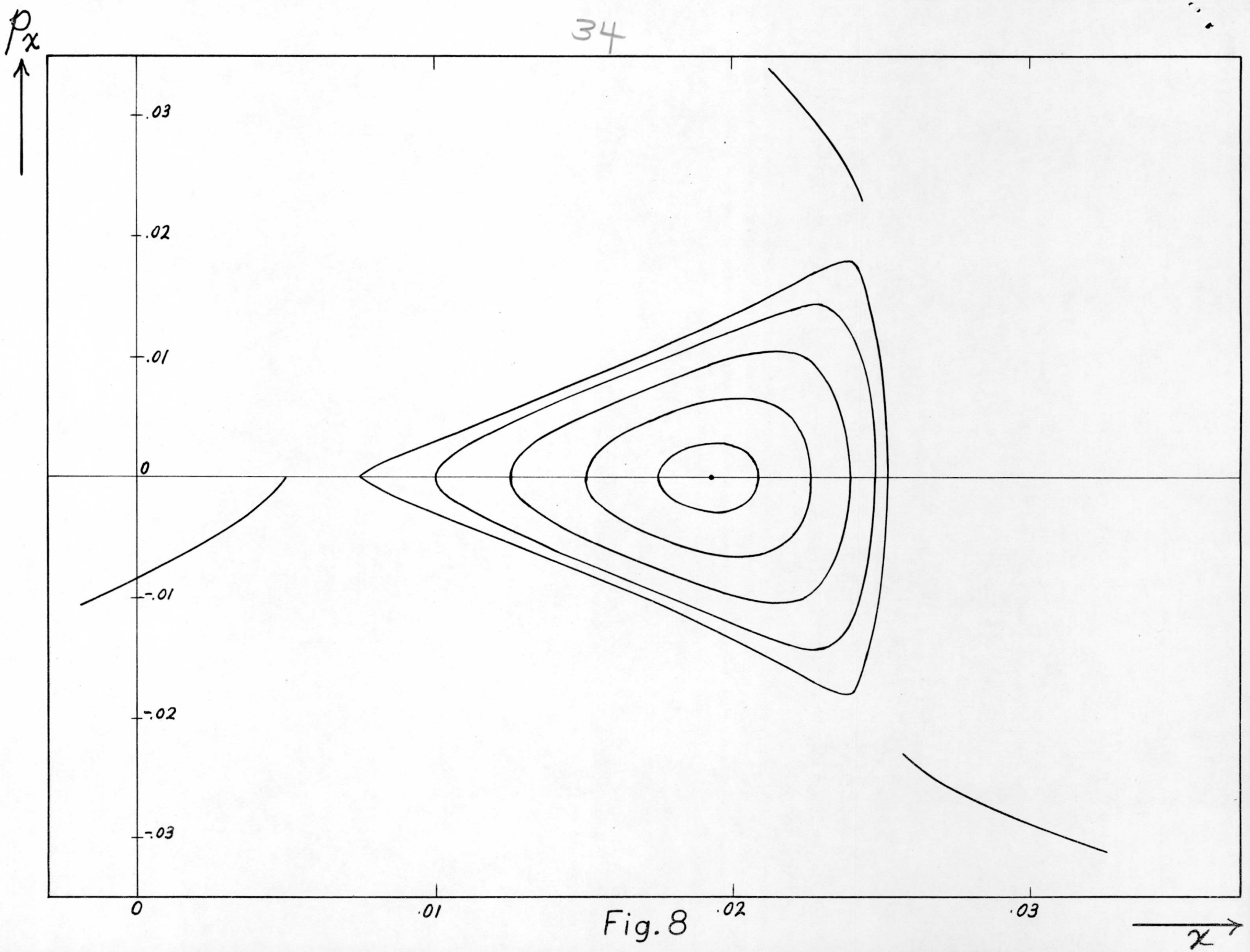

Fig. 8

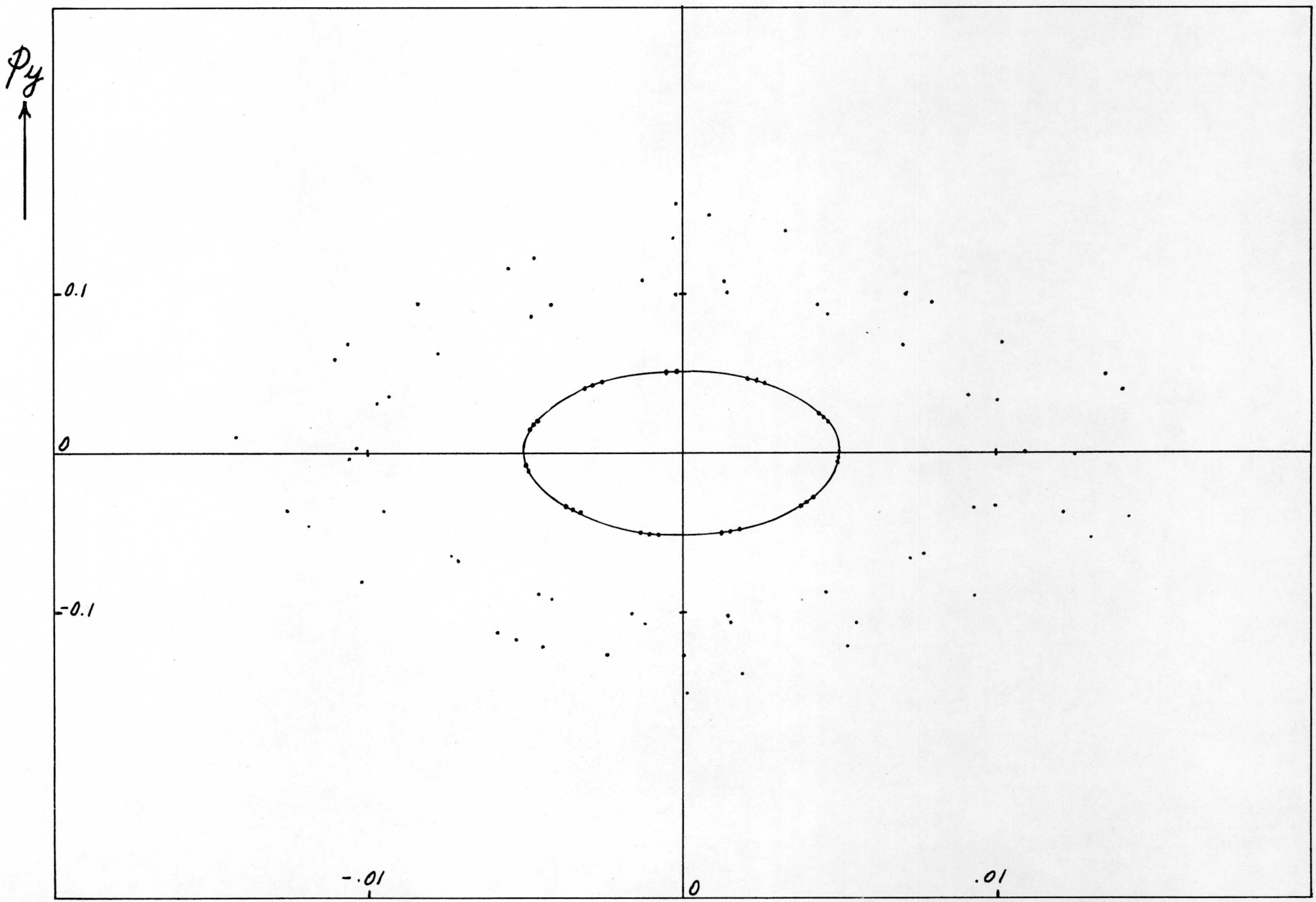

Fig. 9